

## RESEARCH ARTICLE

[View Article Online](#)  
[View Journal](#) | [View Issue](#)

 Cite this: *Inorg. Chem. Front.*, 2024, **11**, 5973

 Received 31st May 2024,  
 Accepted 25th July 2024  
 DOI: 10.1039/d4qi01368a  
[rsc.li/frontiers-inorganic](https://rsc.li/frontiers-inorganic)

# Visible-light-active benzothiadiazole-based MOFs as efficient ROS generators for the synthesis of benzimidazoles and benzothiazoles†

 Hua Liu,<sup>a</sup> Wen-Wen Yi,<sup>\*b</sup> Quan-Quan Li<sup>\*c</sup> and Shu-Ya Zhao<sup>d</sup>

The utilization of reactive oxygen species (ROS) in photochemical synthesis has garnered significant attention owing to their exceptional oxidative capacity under mild conditions. Recently, metal–organic frameworks (MOFs) have been employed to convert molecular oxygen (O<sub>2</sub>) to ROS for photocatalysis. However, visible-light-active MOFs for effective oxygen activation remain scarce. Herein, a simple and effective strategy, linker functionalization, is utilized to immobilize the benzothiadiazole unit inside the UiO-68-type MOF (UiO-68-BTDB). The MOF was applied as the first example generating superoxide radical anions (O<sub>2</sub><sup>•-</sup>) and singlet oxygen (<sup>1</sup>O<sub>2</sub>) for access to benzimidazoles and benzothiazoles in air at room temperature. Recycling experiments were performed to confirm the stability and reusability of UiO-68-BTDB as a robust heterogeneous catalyst.

## Introduction

Reactive oxygen species (ROS) represent highly active molecules that are typically generated during normal oxygen metabolism of aerobic life.<sup>1–3</sup> ROS, with exceptional oxidative capabilities, have presented tremendous potential in diverse applications, including photocatalytic organic transformation and photodynamic therapy.<sup>4–6</sup> Until now, efforts have been made to explore artificial chemical systems that produce ROS under environmentally friendly conditions. Among them, organic dyes and noble metal complexes have been widely utilized as photosensitizers to generate ROS for organic transformations.<sup>7–9</sup> However, most photosensitizers suffer from some restrictions of self-degradation, photobleaching and aggregation-caused quenching (ACQ), thus hindering their progress in photocatalytic reactions.<sup>10–12</sup>

Metal–organic frameworks (MOFs) have garnered significant attention in the applications of photochemical synthesis

for their highly crystalline porous structure and tunability in chemical functionality.<sup>13–15</sup> For visible-light-driven ROS generation, many predesigned organic and metal–organic chromophores are employed as linkers and integrated into MOFs, which is highly helpful to enhance the concentration of photocatalytic sites and avoid their self-quenching within the framework.<sup>16–18</sup> Furthermore, the porous nature of MOFs facilitates the transport and diffusion of ROS, thus enhancing their further interaction with incoming reactants.<sup>19–21</sup> On the other hand, the heterogeneous nature of MOF catalysts confers them with easy separation, enhanced stability, and reusability.

Among various photosensitive compounds, it is well known that benzothiadiazoles with bicyclic electron-deficient skeletons exhibit unique photoelectric properties.<sup>22,23</sup> Specifically, benzothiadiazoles have always served as highly efficient ROS photocatalysts because of their easily improved charge transfer efficiency by designing donor–acceptor–donor (D–A–D) type photosensitizers.<sup>24–26</sup> For example, a series of benzothiadiazole-containing linkers were introduced into the MOF frameworks by the Li group, and the obtained JNU series of MOFs showed photocatalytic activity for aerobic oxidation. Therefore, immobilizing benzothiadiazole units into MOFs may be an effective strategy to convert O<sub>2</sub> to ROS for photocatalytic reactions and is desirable.

Bearing these considerations in mind, 4,4'-(benzo[*c*][1,2,5]thiadiazole-4,7-diyl)dibenzoic acid (H<sub>2</sub>BTDB) was selected as the light-harvester and organic ligand to build a visible-light-active MOF, UiO-68-BTDB. Due to the well-isolated benzothiadiazole chromophore in the framework, the MOF not only retained the visible light absorption of H<sub>2</sub>BTDB, but also

<sup>a</sup>College of Chemical Engineering and Technology, Taiyuan University of Science and Technology, Taiyuan 030024, Shanxi Province, China

<sup>b</sup>School of Environment and Resources, Taiyuan University of Science and Technology, Taiyuan 030024, Shanxi Province, China.  
E-mail: 18404984125@163.com

<sup>c</sup>College of New Energy, Yulin University, Yulin 719000, Shaanxi Province, China.  
E-mail: liquanquan@163.com

<sup>d</sup>College of Chemistry & Materials Science, Northwest University, Xi'an 710127, People's Republic of China

†Electronic supplementary information (ESI) available: Experimental procedures, crystallographic data and other photocatalytic details. See DOI: <https://doi.org/10.1039/d4qi01368a>

produced both singlet oxygen ( $^1\text{O}_2$ ) and superoxide radical anions ( $\text{O}_2^{\cdot-}$ ). UiO-68-BTDB can also be used as a photocatalyst for the photochemical synthesis of benzimidazoles and benzothiazoles. By combining the generation of  $^1\text{O}_2$  and  $\text{O}_2^{\cdot-}$ , UiO-68-BTDB exhibits excellent photocatalytic activity in the visible-light-induced condensation cyclization reaction to synthesize benzimidazoles and benzothiazoles.

## Results and discussion

A Zr(IV)-based MOF, UiO-68-BTDB, with the underlying **fcu** topology, by immobilizing a  $\pi$ -conjugated, electron-deficient, benzothiadiazole-functionalized ligand 4,4'-(benzo[*c*][1,2,5]thiadiazole-4,7-diyl)dibenzoic acid ( $\text{H}_2\text{BTDB}$ ) was synthesized (Fig. 1a).<sup>27,28</sup> Powder X-ray diffraction (PXRD) has been conducted to exhibit its isostructural framework with the parent MOF UiO-68 (Fig. 1b).<sup>29</sup> The existence of the incorporated  $\text{H}_2\text{BTDB}$  linker was further verified by  $^1\text{H-NMR}$  spectroscopy and HRMS of the digested MOF samples (Fig. S1 and S2†).  $\text{N}_2$  sorption measurement at 77 K of UiO-68-BTDB exhibited a type I reversible isotherm, and the Brunauer–Emmett–Teller (BET) surface area was calculated to be  $2484 \text{ m}^2 \text{ g}^{-1}$  (Fig. S3a†). Furthermore, the pore size was determined to be 1.34 nm (Fig. S3b†). Meanwhile, UiO-68-BTDB maintained its structural

integrity after being soaked in different organic solvents for three days (Fig. S4†). Thermogravimetric (TG) analyses demonstrated that UiO-68-BTDB can retain its framework up to  $450 \text{ }^\circ\text{C}$  (Fig. S5†).

The optical and electrical properties were next investigated. As shown in Fig. S6,† UiO-68-BTDB gives emission at 510 nm, and this emission band was ascribed to the  $\pi$ - $\pi^*$  transition of the organic ligand in UiO-68-BTDB. To assess the visible light absorption capacity, the UV-visible diffuse reflectance spectrum was obtained. As shown in Fig. 1c, UiO-68-BTDB displayed a broad absorption ranging from 200 to 600 nm. The optical band gap ( $E_g$ ) of UiO-68-BTDB was calculated to be about 2.55 eV by the Kubelka–Munk (KM) method from Tauc plots (Fig. 1c, inset). To evaluate the conduction band (CB) and the valence band (VB) levels, Mott–Schottky measurements were conducted at frequencies of 500, 750, and 1000 Hz. As shown in Fig. 1d, the CB position was determined to be  $-0.87 \text{ V vs. NHE}$  for UiO-68-BTDB. The VB was thus estimated to be  $1.68 \text{ V vs. NHE}$ . Overall, UiO-68-BTDB has a more negative potential ( $-0.87 \text{ V vs. NHE}$ ) than that for the reduction of  $\text{O}_2$  to the superoxide radical ( $-0.33 \text{ V vs. NHE}$ ), indicating that the MOF catalyst may initiate superoxide radical anion ( $\text{O}_2^{\cdot-}$ ) generation.

To further evaluate the photoelectric properties of the prepared MOF, we explored the charge separation capacity through photocurrent response analysis and electrochemical impedance spectroscopy (EIS). As shown in Fig. 1e, UiO-68-BTDB showed significantly higher photocurrent than the  $\text{H}_2\text{BTDB}$  linker, indicative of effective separation of photogenerated electron–hole pairs. Furthermore, this result was further proved by its relatively smaller radii and lower resistance for charge transfer (Fig. S7†), suggesting that introducing the benzothiadiazole photosensitizer into the MOF is beneficial for the charge separation efficiency. In addition, electron paramagnetic resonance (EPR) tests were performed to investigate its capacity to generate ROS upon visible-light irradiation. As shown in Fig. 2a, in the presence of 2,2,6,6-tetramethylpiperidinoxy (TEMP), the EPR signals observed confirmed the generation of singlet oxygen ( $^1\text{O}_2$ ). Furthermore, the formation of superoxide radical anions ( $\text{O}_2^{\cdot-}$ ) was also indicated by adding 5,5-dimethyl-1-pyrroline N-oxide (DMPO) in the EPR experiments (Fig. 2b).

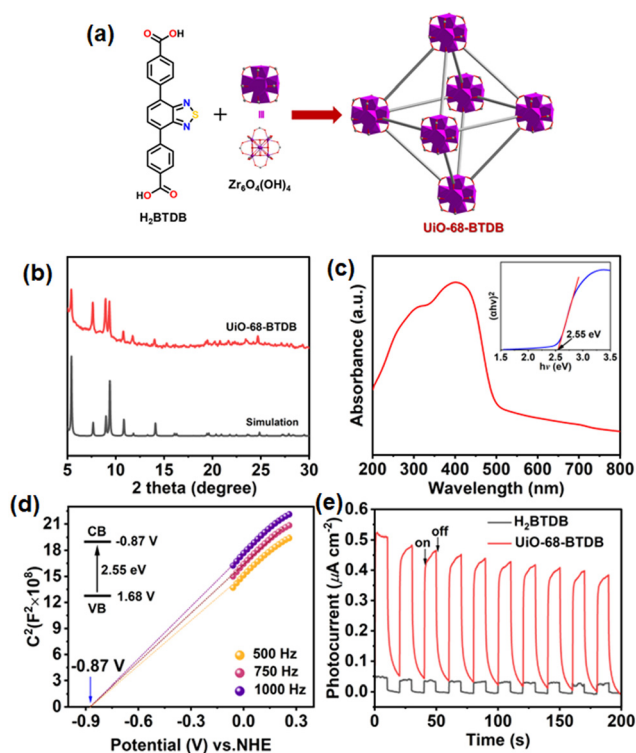


**Fig. 1** (a) Schematic representation of the synthesis of UiO-68-BTDB; (b) PXRD patterns of UiO-68-BTDB. (c) Solid state UV-vis diffuse reflectance spectra (red); inset: Tauc plot of the UiO-68-BTDB (blue); (d) Mott–Schottky plots of UiO-68-BTDB; (e) transient photocurrent responses of UiO-68-BTDB.

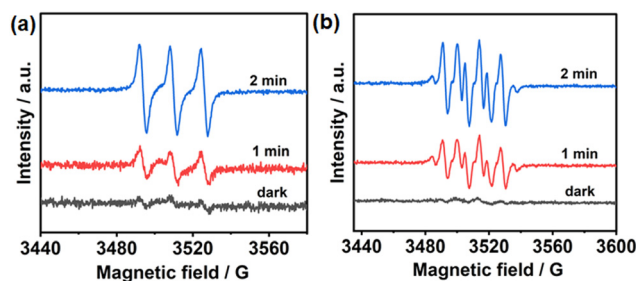


**Fig. 2** (a) EPR detection of  $^1\text{O}_2$  generation with UiO-68-BTDB trapped by TEMP. (b) EPR detection of  $\text{O}_2^{\cdot-}$  generation with UiO-68-BTDB trapped by DMPO.

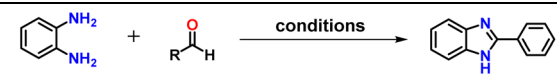
Among heteroaromatic compounds, benzimidazole and benzothiazole derivatives demonstrate potential applications in the pharmaceutical industry and materials science.<sup>30–32</sup> Various approaches have been devoted to synthesize benzimidazoles and benzothiazoles.<sup>32–36</sup> Among them, O<sub>2</sub>-involved oxidation under visible light excitation is considered as a promising one owing to its effective and ecofriendly approach. In terms of the capability of generating <sup>1</sup>O<sub>2</sub> and O<sub>2</sub><sup>•−</sup> of UiO-68-BTDB, we envisioned that photocatalytic condensation cyclization to synthesize benzimidazole and benzothiazole would occur with UiO-68-BTDB as the photocatalyst. As shown in Table 1 (entry 1), the condensation cyclization of *o*-phenylenediamine with benzaldehyde can be achieved in 94% isolated yield with 1 mol% UiO-68-BTDB as the photocatalyst in EtOH and a 10 W blue LED as the light source. Control experiments demonstrated that no product was obtained in the absence of UiO-68-BTDB, a light source, or air (Fig. 3, and Table 1, entries 2–4), indicating the necessity of these reaction parameters. Solvent effects were examined, indicating that EtOH is beneficial for obtaining a high yield of the target product (entries 5–9). Finally, with 1 mol% of UiO-68-BTDB photocatalyst, the

substrates could be efficiently converted to the target product with the highest yield (entries 10–12). Moreover, ligands without a benzothiadiazole unit were also chosen for comparison (Fig. S8†). The obtained UiO-68 was employed as a photocatalyst under similar conditions, and no product was observed (entry 13). A comparison of UiO-68-BTDB with common photocatalysts further demonstrates the superior photocatalytic performance of UiO-68-BTDB (Table S1†).

Under the standard reaction conditions, the substrate scope of aromatic aldehydes was studied to explore the general capability of UiO-68-BTDB as a photocatalyst for the above condensation cyclization reaction. As shown in Table 2, a variety of aromatic aldehydes (with either electron-withdrawing or electron-donating groups) with *o*-phenylenediamine proceeded and afforded the corresponding benzimidazoles with satisfactory yields. It was noted that higher yields of benzimidazole were observed with *para*-substituted benzaldehyde with electron-donating groups (−CH<sub>3</sub> and −OCH<sub>3</sub>) compared to those with electron-withdrawing groups (−NO<sub>2</sub>), demonstrating the significant electronic effect on the reaction.

To investigate the versatility of this method for access to 2-substituted benzothiazole, numerous *para*-substituted ben-

**Table 1** Control experiments of reaction conditions<sup>a</sup>



Entry	Catalyst	Solvent	Amount (mol%)	Yield <sup>b</sup> (%)
1	UiO-68-BTDB	EtOH	1.0	94
2	—	EtOH	1.0	Trace
3 <sup>c</sup>	UiO-68-BTDB	EtOH	1.0	Trace
4 <sup>d</sup>	UiO-68-BTDB	EtOH	1.0	Trace
5	UiO-68-BTDB	DMF	1.0	26
6	UiO-68-BTDB	MeOH	1.0	88
7	UiO-68-BTDB	MeCN	1.0	45
8	UiO-68-BTDB	DCM	1.0	Trace
9	UiO-68-BTDB	THF	1.0	63
10	UiO-68-BTDB	EtOH	0.5	82
11	UiO-68-BTDB	EtOH	1.5	92
12	UiO-68-BTDB	EtOH	2.0	81
13	UiO-68	EtOH	1.0	Trace

<sup>a</sup> *o*-Phenylenediamine (0.2 mmol), benzaldehyde (0.2 mmol), room temperature, a 10 W blue LED, open to air, 3 h. <sup>b</sup> Isolated yields. <sup>c</sup> Conditions in the absence of light. <sup>d</sup> Conditions in the absence of air.

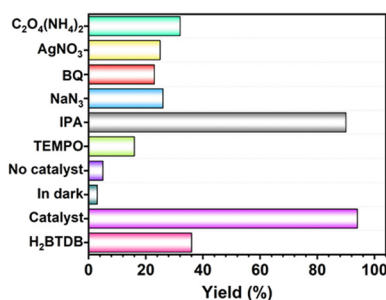
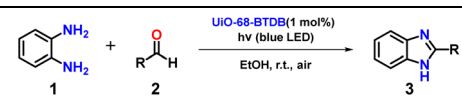


**Fig. 3** Quenching experiments and control experiments.

**Table 2** Photocatalytic condensation cyclization to prepare benzimidazole derivatives<sup>a</sup>



Entry	Substrate	Product	Yield <sup>b</sup> (%)
1			94
2			96
3			96
4			90
5			92
6			98
7			95

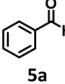
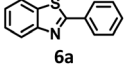
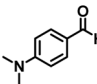
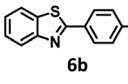
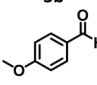
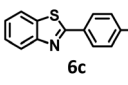
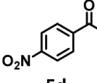
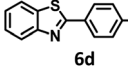
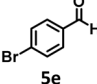
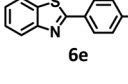
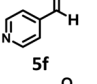
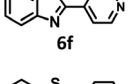
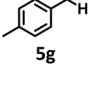
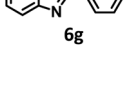
<sup>a</sup> Standard conditions: *o*-phenylenediamine (0.2 mmol), benzaldehyde (0.2 mmol), UiO-68-BTDB, 3 mL EtOH, a 10 W blue LED, room temperature, open to air, 3 h. <sup>b</sup> Isolated yields.

zaldehydes were reacted with *o*-aminothiophenol under the standard conditions to obtain benzothiazoles. As can be seen from Table 3, most substrates gave excellent yields of the target products for only 1.5 h. Overall, the above results showed that UiO-68-BTDB is a general photocatalyst for the synthesis of benzimidazoles and benzothiazoles upon visible light irradiation.

To confirm the heterogeneous nature of UiO-68-BTDB, a series of related experiments were then carried out. As shown in Fig. S9,† the filter experiment showed that the yield of **3a** is unchanged in the next 2 h after removing the catalyst and reacting for 1.5 h. No obvious BTDB<sup>2-</sup> signal in the filtrate was observed in UV-vis spectra, indicating the stability and heterogeneity of UiO-68-BTDB. Additionally, the PXRD pattern of the recovered UiO-68-BTDB after five runs is well consistent with the fresh samples, indicating that it can be recycled for at least five runs without much loss of catalytic efficiency (Fig. S10†). These results commendably demonstrated the heterogeneous nature of UiO-68-BTDB in the photocatalytic condensation cyclization to prepare benzimidazoles and benzothiazoles.

The identification of ROS generated under photocatalytic conditions is essential for elucidating the reaction mechanism

**Table 3** Photocatalytic condensation cyclization to prepare benzothiazole derivatives<sup>a</sup>

Entry	Substrate	Product	Yield <sup>b</sup> (%)
1			97
2			99
3			98
4			93
5			95
6			99
7			96

<sup>a</sup>Standard conditions: *o*-aminothiophenol (0.2 mmol), benzaldehyde (0.2 mmol), UiO-68-BTDB, 3 mL EtOH, a 10 W blue LED, room temperature, open to air, 1.5 h. <sup>b</sup>Isolated yields.

of the condensation cyclization. Thus, the ROS quenching tests were further conducted. As shown in Fig. 3 and Table S2,† when the radical scavenger 2,2,6,6-tetramethylpiperidinyl-1-oxide (TEMPO) was added to the reaction system, the yield of **3a** decreased significantly to 16%, confirming the radical reaction process. The addition of isopropyl alcohol (IPA) had a very little effect on the yield, thus ruling out the presence of <sup>•</sup>OH. After adding NaN<sub>3</sub>, a typical scavenger for <sup>1</sup>O<sub>2</sub>, the reaction yield (26%) was dramatically decreased. The quenched yield (23%) was observed with the addition of the O<sub>2</sub><sup>•-</sup> scavenger *p*-benzoquinone (BQ). Furthermore, the reaction was greatly inhibited when the hole (h<sup>+</sup>) scavenger C<sub>2</sub>O<sub>4</sub>(NH<sub>4</sub>)<sub>2</sub> or electron (e<sup>-</sup>) scavenger AgNO<sub>3</sub> was added. These results suggested that h<sup>+</sup> and e<sup>-</sup> both play a key role during the photocatalysis, and the major working oxygen species here might be <sup>1</sup>O<sub>2</sub> and O<sub>2</sub><sup>•-</sup>. Overall, it can be deduced that the reaction involves two pathways of energy transfer and electron transfer.

According to the above pieces of evidence and literature reports,<sup>32,33</sup> a tentative reaction mechanism for the condensation cyclization to benzimidazole and benzothiazole was proposed. Initially, *o*-phenylenediamine/*o*-aminothiophenol and benzaldehyde are dehydrated to form intermediate **I**, electrons are excited, and charge carriers are separated on UiO-68-BTDB upon visible-light irradiation. Next, as shown in Fig. 4, the generated holes and electrons could initiate the following reactions: holes ( $E_v = 1.68$  V) could capture an electron from intermediate **I** ( $E(I/II) = 0.45$  V)<sup>37</sup> and afford **II**, which then dissociates a proton to give free radical intermediate **III**. The intermediate **III** undergoes cyclization and then reduced by photogenerated electrons to produce **IV**. At the same time, partial singlet electrons transformed into excited triplet electrons *via* intersystem crossing (ISC),<sup>38</sup> thus producing <sup>1</sup>O<sub>2</sub> through energy transfer (ET).<sup>39</sup> Aminal **V**, which has gained a proton from intermediate **IV**, further reacts with <sup>1</sup>O<sub>2</sub> to afford intermediate **VI**. After releasing hydrogen peroxide (H<sub>2</sub>O<sub>2</sub>), the target product is afforded. On the other hand, the photogenerated holes of UiO-68-BTDB oxidize intermediate **I** and further cyclize to intermediate **II'**. Meanwhile, the photogenerated

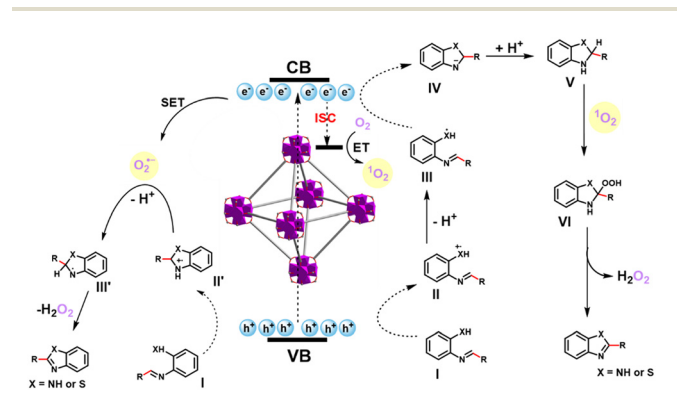


**Fig. 4** Plausible mechanism of UiO-68-BTDB catalyzed the condensation cyclization reaction to synthesize benzimidazoles and benzothiazoles.



electron converts  $O_2$  into  $O_2^{\cdot-}$  via a single electron transfer (SET) mechanism.<sup>40</sup> The target product is afforded by deprotonation of **II'** by  $O_2^{\cdot-}$  and hydrogen abstraction by hydroperoxyl radicals from intermediate **III'**.

## Conclusions

In conclusion, a benzothiadiazole-functionalized ligand ( $H_2BTDB$ ) was rationally designed to construct one UiO-68-type MOF, UiO-68-BTDB. The MOF has a broad adsorption of visible light up to 600 nm and good charge separation efficiency. Merging these merits, UiO-68-BTDB can effectively activate  $O_2$  to  $^1O_2$  and  $O_2^{\cdot-}$  under visible light irradiation. Meanwhile, UiO-68-BTDB is proved to be highly active in condensation cyclization to prepare benzimidazoles and benzothiazoles. Possible dual reaction pathways are proposed for the photocatalytic reaction, including  $^1O_2$  generation via energy transfer and  $O_2^{\cdot-}$  generation via photoinduced charge separation.

## Data availability

Data are available from the authors on reasonable request.

## Conflicts of interest

There are no conflicts to declare.

## Acknowledgements

We gratefully acknowledge the financial support from the Applied Basic Research Programs of Science and Technology Department of Shanxi Province (202303021222245), the Scientific and Technological Innovation Programs of Higher Education Institutions in Shanxi (2023L309), the Yuncheng University Doctoral Research Launch Project (YQ-2023026), and the Taiyuan University of Science and Technology doctoral research start-up fund (no. 20232114).

## Notes and references

- B. C. Dickinson and C. J. Chang, Chemistry and biology of reactive oxygen species in signaling or stress responses, *Nat. Chem. Biol.*, 2011, **7**, 504–511.
- Y. Zhang, J. Pang, J. Li, X. Yang, M. Feng, P. Cai and H.-C. Zhou, Visible-light harvesting pyrene-based MOFs as efficient ROS generators, *Chem. Sci.*, 2019, **10**, 8455–8460.
- E. C. Cheung and K. H. Vousden, The role of ROS in tumour development and progression, *Nat. Rev. Cancer*, 2022, **22**, 280–297.
- W. Huang, B. C. Ma, H. Lu, R. Li, L. Wang, K. Landfester and K. A. I. Zhang, Visible-Light-Promoted Selective Oxidation of Alcohols Using a Covalent Triazine Framework, *ACS Catal.*, 2017, **7**, 5438–5442.
- Z. Zhou, J. Song, L. Nie and X. Chen, Reactive oxygen species generating systems meeting challenges of photo-dynamic cancer therapy, *Chem. Soc. Rev.*, 2016, **45**, 6597–6626.
- Y. Nosaka and A. Y. Nosaka, Generation and detection of reactive oxygen species in photocatalysis, *Chem. Rev.*, 2017, **117**, 11302–11336.
- X. Ding and B.-H. Han, Metallophthalocyanine-Based Conjugated Microporous Polymers as Highly Efficient Photosensitizers for Singlet Oxygen Generation, *Angew. Chem., Int. Ed.*, 2015, **54**, 6536–6539.
- C. K. Prier, D. A. Rankic and D. W. C. MacMillan, Visible Light Photoredox Catalysis with Transition Metal Complexes: Applications in Organic Synthesis, *Chem. Rev.*, 2013, **113**, 5322–5363.
- P. Rana, N. Singh, P. Majumdar and S. P. Singh, Evolution of BODIPY/aza-BODIPY dyes for organic photoredox/energy transfer catalysis, *Coord. Chem. Rev.*, 2022, **470**, 214698.
- X. Ding and B. H. Han, Metallophthalocyanine-based conjugated microporous polymers as highly efficient photosensitizers for singlet oxygen generation, *Angew. Chem., Int. Ed.*, 2015, **54**, 6536–6539.
- I. Pibiri, S. Buscemi, A. Palumbo Piccionello and A. Pace, Photochemically Produced Singlet Oxygen: Applications and Perspectives, *ChemPhotoChem*, 2018, **2**, 535–547.
- Y. Quan, W. Shi, Y. Song, X. Jiang, C. Wang and W. Lin, Bifunctional Metal–Organic Layer with Organic Dyes and Iron Centers for Synergistic Photoredox Catalysis, *J. Am. Chem. Soc.*, 2021, **143**, 3075–3080.
- N.-Y. Huang, Y.-T. Zheng, D. Chen, Z.-Y. Chen, C.-Z. Huang and Q. Xu, Reticular framework materials for photocatalytic organic reactions, *Chem. Soc. Rev.*, 2023, **52**, 7949–8004.
- H. Liu, Q. Li, P. Pan, L. Zhou, B. Deng, S. Zhao, P. Liu, Y. Wang and J. Li, Robust chromophore-integrated MOFs as highly visible-white-light active and tunable size-selective photocatalysts towards benzothiazoles, *Chin. Chem. Lett.*, 2023, **34**, 108562.
- Q. Zhang, Y. Jin, L. Ma, Y. Zhang, C. Meng and C. Duan, Chromophore-Inspired Design of Pyridinium-Based Metal–Organic Polymers for Dual Photoredox Catalysis, *Angew. Chem., Int. Ed.*, 2022, **61**, e202204918.
- H. Liu, Q.-Q. Li, L. Zhou, B. Deng, P.-H. Pan, S.-Y. Zhao, P. Liu, Y.-Y. Wang and J.-L. Li, Confinement of Organic Dyes in UiO-66-Type Metal–Organic Frameworks for the Enhanced Synthesis of [1,2,5]Thiadiazole[3,4-g]benzoimidazoles, *J. Am. Chem. Soc.*, 2023, **145**, 17588–17596.
- Y. Pan, J. Wang, S. Chen, W. Yang, C. Ding, A. Waseem and H.-L. Jiang, Linker engineering in metal–organic frameworks for dark photocatalysis, *Chem. Sci.*, 2022, **13**, 6696–6703.
- K. Wu, X.-Y. Liu, P.-W. Cheng, Y.-L. Huang, J. Zheng, M. Xie, W. Lu and D. Li, Linker Engineering for Reactive Oxygen Species Generation Efficiency in Ultra-Stable

- Nickel-Based Metal–Organic Frameworks, *J. Am. Chem. Soc.*, 2023, **145**, 18931–18938.
- 19 C. T. Buru, M. B. Majewski, A. J. Howarth, R. H. Lavroff, C.-W. Kung, A. W. Peters, S. Goswami and O. K. Farha, Improving the Efficiency of Mustard Gas Simulant Detoxification by Tuning the Singlet Oxygen Quantum Yield in Metal–Organic Frameworks and Their Corresponding Thin Films, *ACS Appl. Mater. Interfaces*, 2018, **10**, 23802–23806.
  - 20 K. Lu, C. He and W. Lin, Nanoscale Metal–Organic Framework for Highly Effective Photodynamic Therapy of Resistant Head and Neck Cancer, *J. Am. Chem. Soc.*, 2014, **136**, 16712–16715.
  - 21 J. Park, D. Feng, S. Yuan and H. C. Zhou, Photochromic metal–organic frameworks: reversible control of singlet oxygen generation, *Angew. Chem.*, 2015, **127**, 440–445.
  - 22 M. Axelsson, Z. Xia, S. Wang, M. Cheng and H. Tian, Role of the Benzothiadiazole Unit in Organic Polymers on Photocatalytic Hydrogen Production, *JACS Au*, 2024, **4**, 570–577.
  - 23 W. Chen, L. Wang, D. Mo, F. He, Z. Wen, X. Wu, H. Xu and L. Chen, Modulating benzothiadiazole-based covalent organic frameworks via halogenation for enhanced photocatalytic water splitting, *Angew. Chem.*, 2020, **132**, 17050–17057.
  - 24 J.-K. Jin, K. Wu, X.-Y. Liu, G.-Q. Huang, Y.-L. Huang, D. Luo, M. Xie, Y. Zhao, W. Lu, X.-P. Zhou, J. He and D. Li, Building a Pyrazole–Benzothiadiazole–Pyrazole Photosensitizer into Metal–Organic Frameworks for Photocatalytic Aerobic Oxidation, *J. Am. Chem. Soc.*, 2021, **143**, 21340–21349.
  - 25 H. Jiang, Y. Wang, C. Li, B. Wang, L. Ma, Y. Ren, Y. Bi, Y. Li, H. Xue and D. Prusky, The effect of benzo-(1,2,3)-thiadiazole-7-carbothioic acid S-methyl ester (BTH) treatment on regulation of reactive oxygen species metabolism involved in wound healing of potato tubers during postharvest, *Food Chem.*, 2020, **309**, 125608.
  - 26 J. Yu, S. Chang, X. Xu, X. He and C. Zhang, Photocatalytic Hydrogen Evolution Based on Nitrogen-Containing Donor–Acceptor (D–A) Organic Conjugated Small Molecules, *ACS Sustainable Chem. Eng.*, 2020, **8**, 14253–14261.
  - 27 H. Liu, S.-Y. Zhao, Q.-Q. Li, X.-S. Li, Y.-J. He, P. Liu, Y.-Y. Wang and J.-L. Li, Linker engineering in UiO-68-type metal–organic frameworks for the photocatalytic thioamide cyclization, *J. Mater. Chem. A*, 2024, **12**, 9527–9531.
  - 28 A. Mallick, A. M. El-Zohry, O. Shekhah, J. Yin, J. Jia, H. Aggarwal, A.-H. Emwas, O. F. Mohammed and M. Eddaoudi, Unprecedented Ultralow Detection Limit of Amines using a Thiadiazole-Functionalized Zr(IV)-Based Metal–Organic Framework, *J. Am. Chem. Soc.*, 2019, **141**, 7245–7249.
  - 29 K. Manna, P. Ji, Z. Lin, F. X. Greene, A. Urban, N. C. Thacker and W. Lin, Chemoselective single-site Earth-abundant metal catalysts at metal–organic framework nodes, *Nat. Commun.*, 2016, **7**, 12610.
  - 30 K. Chakrabarti, M. Maji and S. Kundu, Cooperative iridium complex-catalyzed synthesis of quinoxalines, benzimidazoles and quinazolines in water, *Green Chem.*, 2019, **21**, 1999–2004.
  - 31 B. Chen, C. Zhang, L. Niu, X. Shi, H. Zhang, X. Lan and G. Bai, Biomass-Derived N-doped Carbon Materials with Silica-Supported Ultrasmall ZnO Nanoparticles: Robust Catalysts for the Green Synthesis of Benzimidazoles, *Chem. – Eur. J.*, 2018, **24**, 3481–3487.
  - 32 Z. Li, H. Song, R. Guo, M. Zuo, C. Hou, S. Sun, X. He, Z. Sun and W. Chu, Visible-light-induced condensation cyclization to synthesize benzimidazoles using fluorescein as a photocatalyst, *Green Chem.*, 2019, **21**, 3602–3605.
  - 33 W.-K. An, S.-J. Zheng, H.-X. Zhang, T.-T. Shang, H.-R. Wang, X.-J. Xu, Q. Jin, Y. Qin, Y. Ren, S. Jiang, C.-L. Xu, M.-S. Hou and Z. Pan, s-Tetrazine-functionalized hyper-crosslinked polymers for efficient photocatalytic synthesis of benzimidazoles, *Green Chem.*, 2021, **23**, 1292–1299.
  - 34 S. Samanta, S. Das and P. Biswas, Photocatalysis by 3,6-Disubstituted-s-Tetrazine: Visible-Light Driven Metal-Free Green Synthesis of 2-Substituted Benzimidazole and Benzothiazole, *J. Org. Chem.*, 2013, **78**, 11184–11193.
  - 35 P. Daw, Y. Ben-David and D. Milstein, Direct Synthesis of Benzimidazoles by Dehydrogenative Coupling of Aromatic Diamines and Alcohols Catalyzed by Cobalt, *ACS Catal.*, 2017, **7**, 7456–7460.
  - 36 R. Zhang, Y. Qin, L. Zhang and S. Luo, Oxidative Synthesis of Benzimidazoles, Quinoxalines, and Benzoxazoles from Primary Amines by ortho-Quinone Catalysis, *Org. Lett.*, 2017, **19**, 5629–5632.
  - 37 W.-K. An, S.-J. Zheng, Y.-N. Du, S.-Y. Ding, Z.-J. Li, S. Jiang, Y. Qin, X. Liu, P.-F. Wei, Z.-Q. Cao, M. Song and Z. Pan, Thiophene-embedded conjugated microporous polymers for photocatalysis, *Catal. Sci. Technol.*, 2020, **10**, 5171–5180.
  - 38 Intersystem Crossing (ISC) refers to a non-radiative leaping process in which the electrons of a molecule in an excited state undergo a spin reversal, resulting in a change in the multiplicity of the molecule. The process involves the crossing of a molecule from an excited singlet state to an excited triplet state.
  - 39 Energy Transfer (ET) refers to the phenomenon of energy being passed, transferred, or exchanged between molecules through collisions.
  - 40 Single Electron Transfer (SET) refers to a reaction mechanism in which a single electron is transferred between different species during a fundamental reaction step on the reaction coordinate. This process typically involves the movement of an electron from an electron-rich species to an electron-poor species, often resulting in the change of oxidation states of the reactants and the possible formation of radical intermediates.